

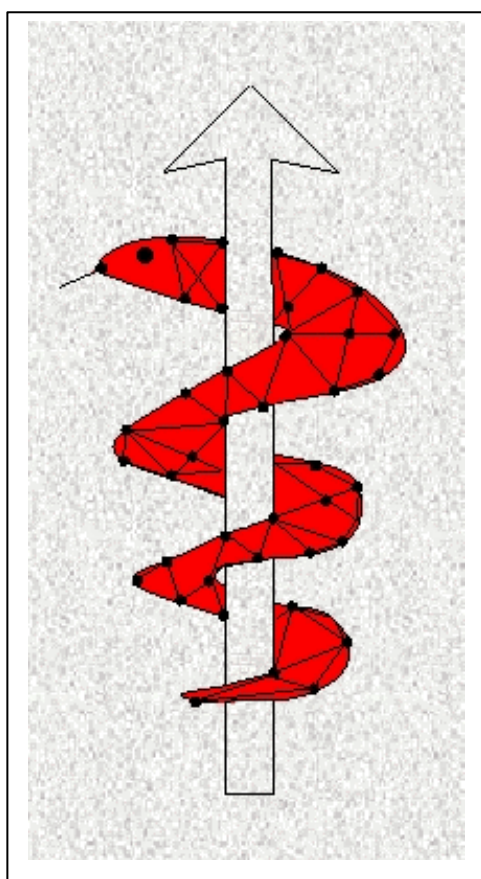


The IST Programme Project No. 10378

SimBio

SimBio - A Generic Environment for Bio-numerical Simulation

<http://www.simbio.de>



Deliverable D2b Release Notes on Preliminary MD Release

Status:	final
Version:	1.0
Security:	Public
Responsible:	CNRS
Authoring Partners:	BMZ, ESI, MPI, USFD

The SimBio Consortium :

NEC Europe Ltd. – UK
A.N.T. Software – The Netherlands
CNRS-DR18 – France
Sheffield University – UK

MPI of Cognitive Neuroscience – Germany
Biomagnetisches Zentrum Jena – Germany
ESI Group – France
Smith & Nephew - UK

Contents

1	INTRODUCTION.....	4
2	BIO-MECHANICAL MATERIAL DATA ACQUISITION - SMALL SAMPLE.....	4
2.1	GENERAL APPROACH.....	5
2.2	BRAIN WHITE MATTER.....	5
2.2.1	<i>Methods</i>	5
2.2.2	<i>Results</i>	8
2.2.3	<i>Summary</i>	11
2.3	MENISCUS.....	11
2.3.1	<i>Methods</i>	11
2.3.2	<i>Results</i>	13
2.3.3	<i>Summary</i>	15
3	BIO-MECHANICAL MATERIAL DATA ACQUISITION - MRSI.....	16
3.1	MAGNETIC RESONANCE STRAIN IMAGING MRSI - THE METHOD.....	16
3.2	THEORETICAL MODEL - CONSTITUTIVE EQUATION.....	16
3.3	MAGNETIC RESONANCE STRAIN IMAGING – REALISATION.....	16
3.3.1	<i>In vitro embedding techniques for soft tissue</i>	16
3.3.2	<i>Construction of a deformation-cube</i>	17
3.3.3	<i>Embedding of complex structures ex vivo</i>	17
3.4	ADVANCED TECHNIQUES FOR IN VIVO EVALUATION OF TISSUE MOVEMENT.....	18
3.4.1	<i>MRI acquisition of dynamic deformation</i>	18
3.4.2	<i>Phase contrast sequences</i>	18
3.4.3	<i>Time resolving phase contrast sequences</i>	18
4	BIO-ELECTRICAL MATERIAL DATA ACQUISITION.....	20
4.1	MR TECHNIQUE CALLED DIFFUSION TENSOR IMAGING (DTI).....	20
4.2	COMPUTATION OF TISSUE CONDUCTIVITIES FROM MEG/EEG/ECOG MEASUREMENTS.....	20
4.3	DIFFUSION TENSOR SCANS.....	20
4.4	DEVELOPMENT OF AN INDIVIDUAL CONDUCTIVITY TENSOR MAP.....	21
5	BIO-MATERIAL DATABASE.....	21
5.1	LITERATURE-BASED DATA.....	21
5.2	DATABASE.....	21
5.2.1	<i>Data presentation</i>	21
5.2.2	<i>Data encoding</i>	22
6	LITERATURE.....	23
7	MECHANICAL TISSUE PROPERTIES.....	25
7.1	SOFT TISSUE.....	25
7.2	HARD TISSUE.....	27
8	ELECTRICAL TISSUE PROPERTIES.....	28
8.1	SOFT TISSUE.....	28
8.1.1	<i>Brain matter, spinal cord, and cerebellum</i>	28
8.1.2	<i>Muscle</i>	28
8.1.3	<i>Fat</i>	29
8.1.4	<i>Scalp</i>	29
8.2	BONE.....	29
8.3	FLUIDS.....	29
8.3.1	<i>Blood</i>	29
8.3.2	<i>Cerebrospinal fluid</i>	29

Table of figures

Figure 1: Typical sample shown from two different angles (90°).....	6
Figure 2: Universal testing machine modified to perform compression experiments on cylindrical soft tissue samples. The left side shows an overview of the machine with integrated balance, the right hand side gives the balance with climate chamber and piston.	7
Figure 3: Controlled climate chamber for traction/compression experiments:	7
Figure 4: Stress/strain curves for perpendicular samples.....	8
Figure 5: Stress/strain curves for parallel samples.....	9
Figure 6: Comparative graphic: Median stress-strain curves for parallel (lower curve) and perpendicular samples (upper curve), based on regression curves.....	9
Figure 7: Ratio of the median of the graphs for perpendicular and parallel samples.....	9
Figure 8: Stress/strain curves for perpendicular samples harvested from an undisturbed brain.	10
Figure 9: Median stress-strain curves for perpendicular samples harvested from brains from cows sacrificed by blow in the head (triangle) and by the brain not interfering throat cutting (circle).	10
Figure 10: Samples have been cut as parallelepipeds from the central third of every meniscus (lateral or medial) to obtain rectangular probes for traction tests, from which the central part was cut afterwards to obtain cubic samples for the compression anisotropy experiments.....	11
Figure 11: A second type of cubic samples where taken for comparison reasons from the anterior or posterior part of every meniscus (medial or lateral) and used for compression anisotropy tests.	12
Figure 12:•Time depended deformation of samples of meniscus tissue. Samples are placed: For traction tests between two jaws. For compression tests between two plates.....	12
Figure 13: Image as taken during a traction experiment.	13
Figure 14: Stress/strain curves acquired by compression of samples from the posterior part of lateral meniscuses in direction D1.....	13
Figure 15: Median of the results of the 6 experiments presented in the figure above.	14
Figure 16: Comparative graphic : Median stress-strain curves for the 3 direction.	14
Figure 17: Ratio of the median of the graphs for perpendicular and parallel samples.....	14
Figure 18: <i>Reconstruction of part of a gel-embedded bovine brain in the relaxed and deformed state.</i>	17
Figure 19: Heart action synchronized amplitude images of the aorta abdominalis during the last quarter of the heart cycle.....	19
Figure 20: Heart action synchronized phase images of the aorta abdominalis during the last quarter of the heart cycle.	19
Figure 21: Structure of datase in ‘Access’.	22

Table of tables

Table 1: Mechanical properties of tissues of the neuro-cranium regarding linear elasticity...	25
Table 2: Mechanical properties of tissues of the neuro-cranium regarding linear viscoelasticity.....	25
Table 3: Special data of mechanical properties of tissues of the neuro-cranium	26
Table 4: Mechanical properties of articular cartilagec	27
Table 5: Mechanical properties of meniscus	27
Table 6: Mechanical properties of cortical and cancellous bone	27
Table 7: Resistivity of brain white matter	28
Table 8: Resistivity of brain grey matter	28
Table 9: Resistivity of spinal cord	28
Table 10: Resistivity of cerebellum.....	28
Table 11: Resistivity of muscle	28
Table 12: Resistivity of fat	29
Table 13: Resistivity of scalp	29
Table 14: Resistivity of bone	29
Table 15: Resistivity of blood	29
Table 16: Resistivity of cerebrospinal fluid	29

1 Introduction

The central objective of the SimBio project is the improvement of clinical and medical practices by the use of numerical simulation for bio-medical problems. Modelling and simulations for biomedical applications is a demanding task, which requires an adequate and reliable material database to achieve meaningful results. The 'Compilation of the Material Database' (workpackage 2) is therefore an important module providing the basis for the generic SimBio environment. It provides the input for the WP 'Geometric Model Generation', which is the basis for all further WP's.

Since projected applications include as well mechanical as electrical simulations the database has to include detailed data about both these tissue properties. One might argue that there is already a large amount of data available in literature, so it is not necessary to generate additional. Anyway due to the problems mentioned briefly in the following there is even so a lack of data obtained under boundaries as related to real life situations i.e. body temperature, humidity, different types and degrees of pre-deformation. E.g. the ambitious *WSU Brain Injury Model* takes into account single values for the 'homogeneous' tissue types: brain, CSF, membrane, and skull only neglecting so far the different types of brain matter as well as eventual tissue anisotropy etc.

This report is focused on the description of our work concerning the generation of mechanical and electrical properties data from tissue as near to the living state as possible taking into account eventual inhomogeneity, nonlinearity, and anisotropy. The report summarises the methodological progress made so far as well as preliminary and first results as concerning the meniscus and brain tissue, respectively.

The database as presented in the 'Appendix' presents mainly information collected from literature about human tissue properties and the experimental approaches established to gather this data. As mentioned already available existing knowledge and data is in no terms sufficient for simulations of living systems. So the main part of the work in this workpackage has to be the development of appropriate experimental set-ups and execution of the according experiments to generate the needed base of normal, physiological data.

Furthermore the project aims to model electrical and mechanical properties of human tissue of individuals for diagnostic and therapeutic purposes, which means that applied methods need to be non destructive and as non invasive as possible. For this reasons magnetic resonance strain imaging (MRSI) and diffusion tensor imaging (DTI) have been chosen as the basic approaches. Both methods basically rely on magnetic resonance imaging (MRI) and have been developed very recently. Their major advantage in comparison to previous methods is the possibility to make investigations in-situ and *in-vivo*. Data acquired and evaluated in this manner provide real life information for the envisaged models and simulations in contrast to the so far mainly effected *ex-vivo* measurements.

Bio-mechanical material data acquisition - small sample

Detailed knowledge about individual material behaviour of human tissue will be measured, calculated and included in the material database. Parallel to acquiring new material knowledge by applying innovative magnetic resonance techniques, data of material properties are collected from literature. Particular features required by the SimBio evaluation applications will be given priority.

Steps in realisation will be:

- data extraction from literature,
- small sample measurement using a universal testing machine
- Magnetic Resonance Strain Imaging (MRSI) of *ex vivo* coated tissues samples
- MRSI experiments with isolated ex-vivo organs: brains

- MRSI *in vivo*: strains induced *in-vivo* for evaluation of *in vivo* material properties.

2.1 General approach

For the biomechanical part of the material data generation a stepwise approach will be realised:

The first step is the extraction of a general material database from literature, which provides the basis for first simulations. Then direct measurement of mechanical properties of small tissue samples is mandatory since an important step in developing the MRSI technique is evaluating its performance. For this evaluation, an alternate and reliable way of measuring tissue mechanical properties is needed. There are numerous advantages of having a device that can measure these properties of small tissue samples. The most important of which might be the possibility to perform first investigations in anisotropy properties if tissue samples are obtained in an appropriate way. A method to investigate small samples of soft tissue as harvested by biopsy in clinical routine has been established to provide first evaluations of anisotropy and nonlinearity as well as the establishment of a calibration tool for the following techniques.

MR Strain Imaging (MRSI) is a method recently invented and until now only applied to some isolated *ex-vivo* organs as in gel embedded kidneys. So here first experimental steps will be the generation of relevant data by determining material properties of isolated *ex-vivo* brains, parts, entire, and menisci, respectively [Che98, Eme95, Oph99].

In the final step, *in-vivo* investigations are planned to perform *in-vivo* based investigations by inducing defined strain and evaluating the resulting deformation *in situ*. This third step in material properties acquisition will be the most innovative, advanced, and demanding.

The degree of realisation achievable during the runtime of the project will depend on the progress, which is possible in the development of the method. In any case, '*in-vivo* MRSI' will give us directly the mechanical property information we need to realise the goal of our project: to combine the individual geometrical, mechanical, and properties of an individual patient and to introduce them into the individual simulations.

2.2 Brain white matter

White matter is formed by axon fibres, which are oriented in parallel and which are accompanied by glia cells. To investigate the mechanical properties of this type of brain material we developed and performed methods as described in the following.

2.2.1 Methods

2.2.1.1 Types of samples

To achieve good accuracy, the standard clinical procedure of biopsy is used to harvest the samples. The cylindrical samples are taken by standard biopsy punches of 6mm diameter. To investigate the expected anisotropy of the white matter two different types of samples have been taken.

- Firstly samples have been taken by biopsy punch oriented in parallel to the axon fibres, which means fibres in parallel to the axis of symmetry of the cylindrical sample and
- secondly samples where the fibres are oriented perpendicular to this axis.

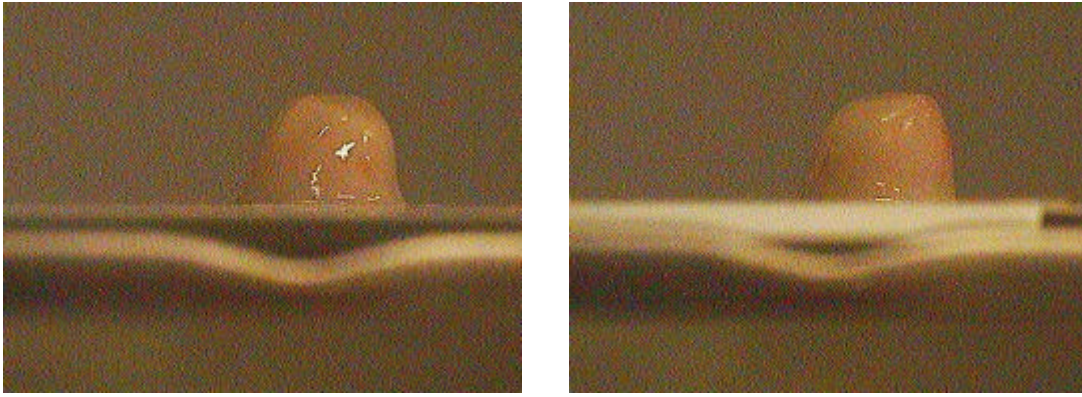


Figure 1: Typical sample shown from two different angles (90°)

2.2.1.2 Types of brain

Experiments have been performed using two different types of brains according to the type of sacrificing of the animals.

The first and so far the major part of experiments have been done using samples as harvested from animals sacrificed by the standard procedure used in slaughter houses. This procedure is also mentioned in most literature and means that the animals are sacrificed by a blow at or even inside the head. Due to the availability we had to use in the beginning brains of this type only, despite the disturbances and changes in mechanical properties of the brain, which might be due to this procedure. So we performed experiments with the two types of samples parallel and perpendicular ones to investigate anisotropy of white brain matter.

The second type of brain is undisturbed by the sacrificing procedure since the animals throat is cut as demanded by several religions. Future experiments will be performed mainly with this type of brains since it turned out that the blow obviously alters brain tissue properties as shown below. Due to the restricted availability we have until now been able to perform experiments using this type of brains for perpendicular samples only.

2.2.1.3 Sample Harvesting

To harvest the samples of brain tissue needed to perform the projected experiments we worked together with the local slaughterhouse. The brains have been taken from cows, sacrificed in the normal routine for nutrition purposes, where the brain is not used. The cows have been aged 24 (4x) and 30 (2x) months respectively. Directly after standard sacrificing of the animals the head has been used in place throughout the first hour after death. The brains harvested have been stored in physiological buffer (saline water, 0.9%) in special hermetically closed boxes.

If possible the brains have been evaluated immediately - the same day, if not, after refrigeration latest within the next 36 h after the animals death.

2.2.1.4 Experimental Setup



Figure 2: Universal testing machine modified to perform compression experiments on cylindrical soft tissue samples. The left side shows an overview of the machine with integrated balance, the right hand side gives the balance with climate chamber and piston.

A system capable of accurate measurements on small (~0.4 cc) cylindrical tissue samples has been integrated in our commercial traction machine.

Deformations are produced by lowering a circular piston, with a radius much bigger than the sample radius, onto the centre of the sample. Deformation is applied and evaluated by routines integrated in the traction machine. The actual force acting on the tissue cylinder is measured by the balance, which in the actual version is read out interactively, automatization is in preparation.

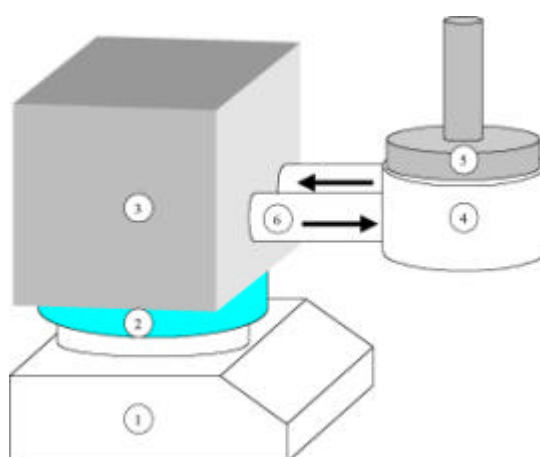


Figure 3: Controlled climate chamber for traction/compression experiments:

- | | |
|-------------------------------|---|
| 1. Controlled heater | 2. Water reservoir (69°C) |
| 3. Moist air reservoir (100%) | 4. « Moist chamber » containing samples |
| 5. Piston of testing machine | 6. Air circulation |

2.2.1.5 Experimental protocol

Cylindrical samples were harvested from randomly chosen locations in white matter regions in perpendicular and parallel direction as related to the direction of the axon fibres, respectively. Appropriate samples are stored in physiological buffer in the refrigerator until use ($\Delta t < 10\text{h}$).

Directly before executing the experiment the sample was positioned in the climate chamber for 15 minutes to equilibrate. The actual geometry of the sample was determined on basis of pictures of a numerical camera.

During the experiment a quasi-static increase of compression (0.5 mm/min) was applied. The according pressure was measured by the integrated balance and read out every 15 s.

2.2.1.6 Data evaluation

Under the described circumstances the investigated white matter brain tissue can be taken to be incompressible ($V = \text{const.}$). The presented stress/strain curves have been obtained under this hypothesis.

Therefore the results of an experiment are firstly into a force/displacement diagram, which is then converted which makes the slightly different geometries of different experiments comparable. So in principal averaging becomes possible. Anyway the previously identical deformation distances (abscissa) become different from experiment to experiment due to their conversion into relative strain values. So the following averaging procedure is applied. The original graphs are fitted by polynomial of third degree, which showed all a regression coefficient of at least 0,99. These polynomials were averaged for all samples. The according graphs are presented with their SED for 30 representative points. Where more appropriate the median is given.

2.2.2 Results

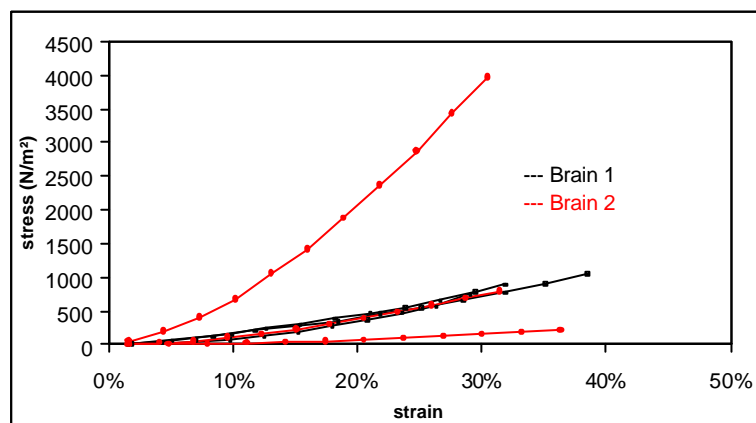


Figure 4: Stress/strain curves for perpendicular samples

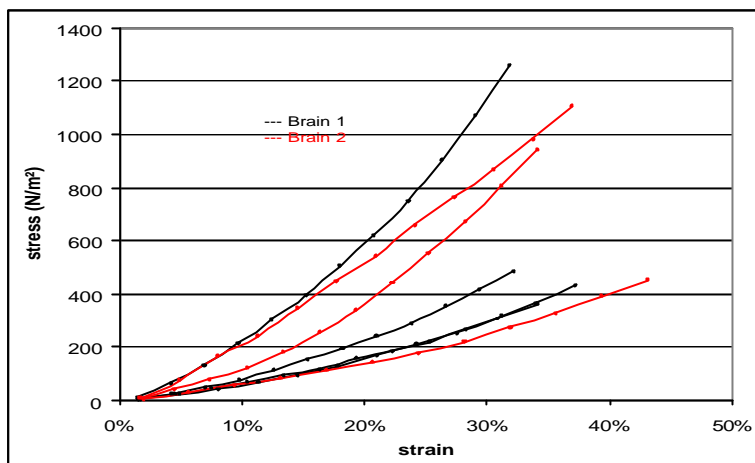


Figure 5: Stress/strain curves for parallel samples

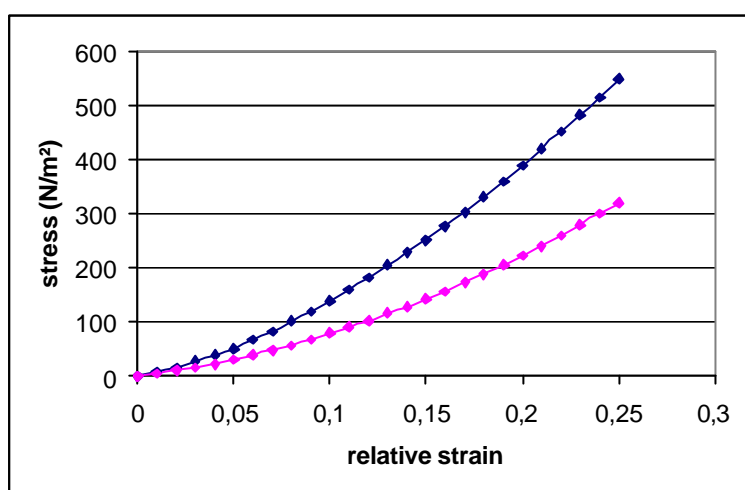


Figure 6: Comparative graphic: Median stress-strain curves for parallel (lower curve) and perpendicular samples (upper curve), based on regression curves

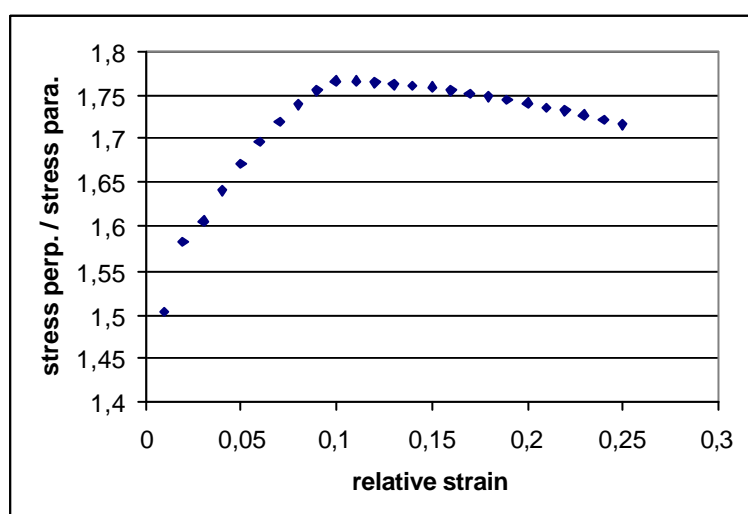


Figure 7: Ratio of the median of the graphs for perpendicular and parallel samples.

Fig. 7 demonstrates the clear cut anisotropy which is to be find in white matter brain material and which is up to 10% strain dependent i.e. increasing with strain for to exhibit than in a wide range a round about 1.7 times higher strain resistance perpendicular to axon fibres than in parallel. These are the results from our measurements with fresh brains of cows which have been sacrificed by a blow.

After realizing the drawback of using brains disturbed by the sacrificing we started the ongoing experiments on brains of cows sacrificed by throat cutting. Results of the first set of experiments performed with this kind of samples are given in Figure 8

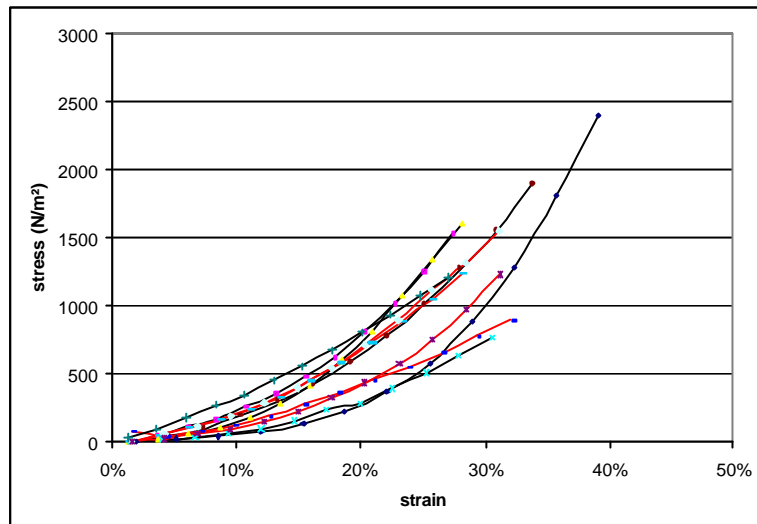


Figure 8: Stress/strain curves for perpendicular samples harvested from an undisturbed brain.

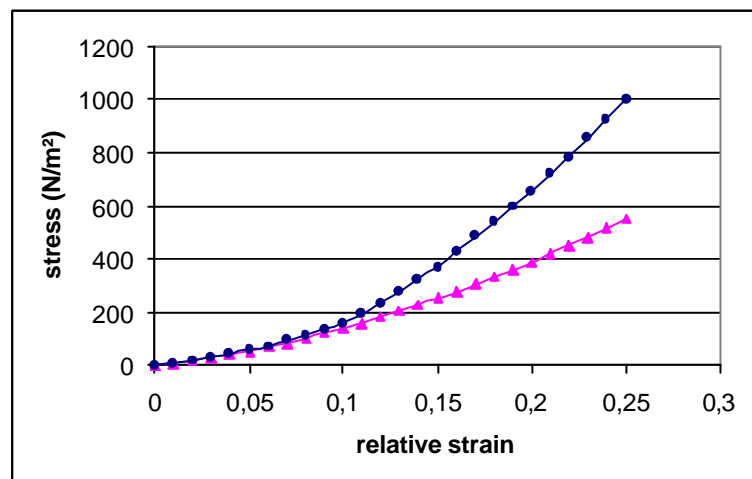


Figure 9: Median stress-strain curves for perpendicular samples harvested from brains from cows sacrificed by blow in the head (triangle) and by the brain not interfering throat cutting (circle).

To be able to compare samples from the different brains we performed stress-strain experiments with perpendicular samples taken from the white matter of the two types of brain. Figure 9 shows the stress/strain curves as determined for samples of perpendicular direction for the two. Again for 10% of strain there is a change in properties to be found. Up to this limit no significant difference in the investigated mechanical properties can be stated, while from there on the undisturbed brain shows an increase in strain resistance, which is not to be found for the blow-altered brain.

From these results it can already be stated that the application of blows changes mechanical properties of brain white matter even if macroscopically no changes are detectable.

2.2.3 Summary

2.2.3.1 Elasticity

We found a Young's modulus for white matter bovine brain tissue in perpendicular to the axon fibres of about 6000 N/m^2 under the following boundaries: deformation by compression with 0.5 mm/min , for a relative strain from 0.1 up to 0.25, in an environment of $34^{\pm} 2^{\circ}\text{C}$ temperature, 100% humidity, samples taken from fresh brain in between 36h.

2.2.3.2 Anisotropy

For bovine brains altered by a blow we found for the white matter a pronounced higher elasticity in the direction in perpendicular to the fibres than in parallel. The ratio increases from 1.5 to 1.75 for relative strains from 0 to 0.1 and rests than nearly constant at 1.7 up to 0.25 relative strain. These values have to be verified for unaltered brains. Anyway, since blow like disturbances should destroy structures one would expect an even bigger anisotropy for the unaltered brain.

2.3 Meniscus

Preliminary experiments have been performed so far, aiming to establish and to verify our experimental approach and to obtain first qualitative results.

2.3.1 Methods

2.3.1.1 Types of samples

Small tissue samples have been harvested from porcine menisci using standard clinical equipment. To investigate the expected anisotropy of the white matter two different types of sample geometries have been taken.

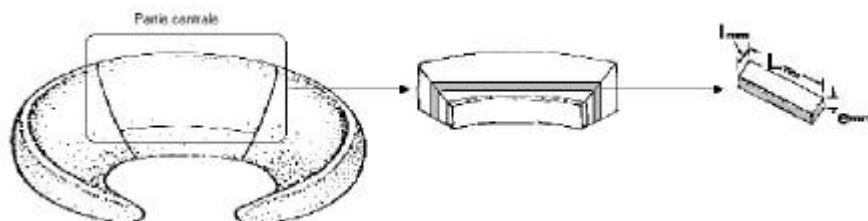


Figure 10: Samples have been cut as parallelepipeds from the central third of every meniscus (lateral or medial) to obtain rectangular probes for traction tests, from which the central part was cut afterwards to obtain cubic samples for the compression anisotropy experiments.

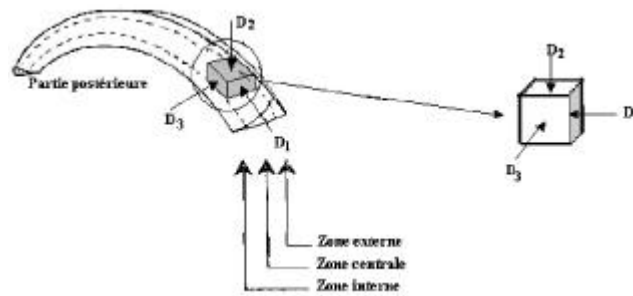


Figure 11: A second type of cubic samples were taken for comparison reasons from the anterior or posterior part of every meniscus (medial or lateral) and used for compression anisotropy tests.

2.3.1.2 Sample harvesting

The samples have been taken from animals of the race Large White aged 10 ± 1 weeks and of a weight of 35.4 ± 4.5 kg. Knees have been taken in between 24h after sacrificing and the menisci have been dissected, stored in physiological buffer (Ringer's solution) and frozen (-20°C) until examination.

2.3.1.3 Set-up

In principal the same set-up type of universal testing machine has been used as for the brain experiments, except that there has so far not been a climate chamber.

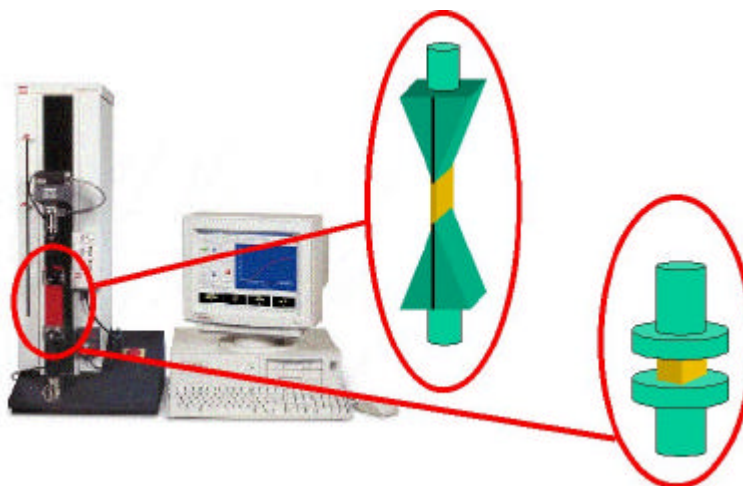


**Figure 12: •Time depended deformation of samples of meniscus tissue. Samples are placed:
For traction tests between two jaws.
For compression tests between two plates**

2.3.1.4 Experimental protocol

The samples were harvested as described above. Appropriate samples were stored in physiological buffer in the refrigerator until use.

Directly before executing the experiment the sample was positioned in the testing machines and allowed to equilibrate to room temperature climate chamber for 15 minutes. The actual geometry of the sample was determined on basis of pictures using a digital camera.

During the experiment a quasi-static increase of traction/compression was applied. The pressure applied to the specimen was directly measured by the traction machine. The according deformation is enregistered by pictures taken during the experiment via a numerical camera.



Figure 13: Image as taken during a traction experiment.

2.3.1.5 Data evaluation

For the traction experiment a numerical camera was synchronized with the testing machine. Pictures were taken during the experiment and were evaluated afterwards semi automatically to determine the deformation effected on the sample part of interest, which is marked by colour dots. The applied forces were automatically measured and enregistered by the machine.

For the compression experiments this was done automatically for both force and deformation. The presented stress/strain curves have been obtained under this hypothesis.

Therefore the results of an experiment were firstly presented by a force/displacement diagram, which was then converted which makes the slightly different geometries of different experiments comparable. The averaging was done in the same manner as already discussed in the 'brain' part.

2.3.2 Results

Experiments have been performed as described above. Exemplary results of a series of experiments are given in Fig.X. for cubes harvested from the posterior part of lateral menisci, which have been compressed in the principal directions.

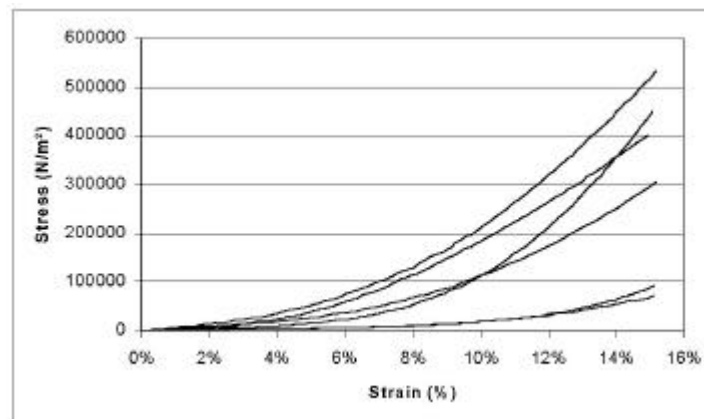


Figure 14: Stress/strain curves acquired by compression of samples from the posterior part of lateral meniscuses in direction D1.

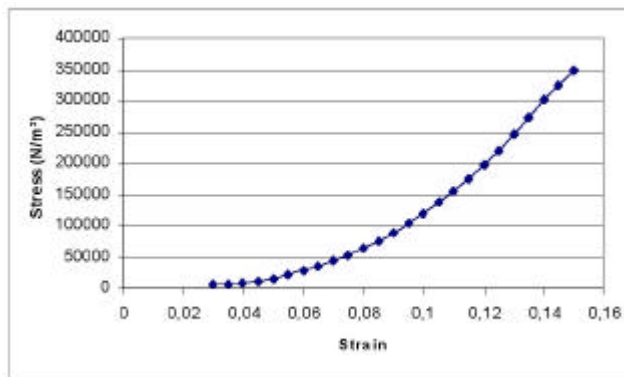


Figure 15: Median of the results of the 6 experiments presented in the figure above.

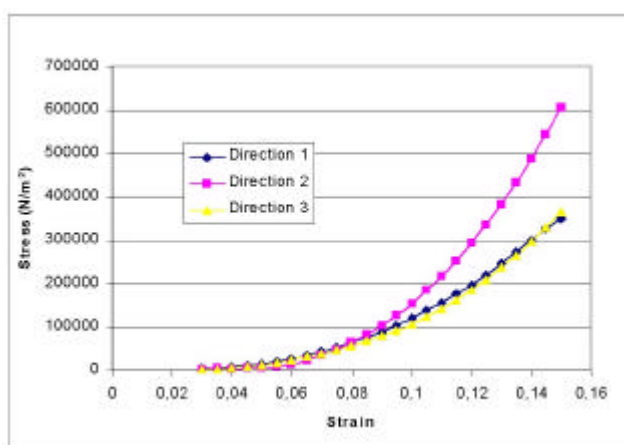


Figure 16: Comparative graphic : Median stress-strain curves for the 3 direction.

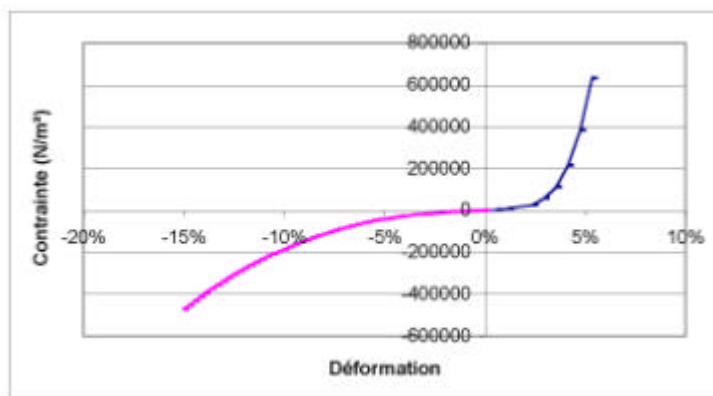


Figure 17: Ratio of the median of the graphs for perpendicular and parallel samples.

2.3.3 Summary

2.3.3.1 Elasticity

Figure 17 shows the result of a preliminary combined traction-compression experiment performed as described above in direction D1. A clear cut difference in visco-elastic behaviour can be stated for the two types of loads, where there is a much higher resistance against elongation than against compression to be found.

2.3.3.2 Anisotropy

The preliminary results presented in Fig. 16 show that there seems to be for the meniscus a plane of isotropy regarding the visco-elastic properties as determined by our experimental protocol while in perpendicular starting from a relative strain of 0.08 on an increasing anisotropy can be stated as related to the other directions.

3 Bio-mechanical material data acquisition - MRSI

3.1 Magnetic Resonance Strain Imaging MRSI - the method

Until now strain imaging techniques have been applied for some isolated 'in vitro' organs (kidneys) only [Erk98, Eme95]. So we aim to set-up this technique for the "in-vivo brain", which should provide detailed knowledge of material properties of 'in place' substructures in the brain in general.

Furthermore the projected 'advanced in vivo strain imaging' technique of patients brain will provide most important insights in individual mechanical brain properties and processes for diagnostics and therapy. Development and installation of this method will be a demanding part of the project and at the moment it is unforeseeable which state of realisation will be reachable during the runtime of the project.

3.2 Theoretical model - Constitutive equation

To evaluate mechanical properties of a body on the basis of stress-strain experiments firstly a constitutive equation has to be established. A general approach can be developed as follows: The general equation of equilibrium of a body is given by:

$$\sum_{n=1}^3 \frac{\partial \mathbf{s}_{ij}}{\partial x_j} + f_i = 0, \quad i = 1,2,3$$

Stress-strain relation of compressible media can be written

$$\mathbf{s}_{ij} = \left(K - \frac{2}{3} G \right) \mathbf{q} \mathbf{d}_{ij} + 2G \mathbf{e}_{ij}$$

Stress-strain relation of incompressible media:

$$\mathbf{s}_{ij} = p \mathbf{d}_{ij} + 2G \mathbf{e}_{ij}$$

In our approach we aim to establish a constitutive modelling as presented by Miller and Cinzei (1997) for investigation of brain tissue by a compression machine with an extension comparable to the experimental set up published by et al. []for shear measurements. This will enable us to apply the above presented equation for compressible media.

3.3 Magnetic Resonance Strain Imaging – Realisation

The following steps have to be taken to realise and apply the MRSI-method.

3.3.1 In vitro embedding techniques for soft tissue

To develop a appropriate techniques for the coating of isolated organs, the biological tissue, a material has to be chosen which fulfils the following demands:

- neutral in regard to living tissue,
- perfect coating in the liquid phase,
- short time polymerisation,
- no heating up during polymerisation,
- mechanical properties nearly the same as for the investigated tissue.

We found this material thanks to information provided by Haribo Co., which as well provided samples of different compositions of the finally chosen gelatine which origin can be porcine or bovine. By adding varying quantity of glucose syrup one can change the properties of this embedding material.

3.3.2 Construction of a deformation-cube

So far a simple device has been set up which allows to apply a static deformation to a gelatine coated organ inside the MRI machine during image acquisition. The apparatus has been tested in first experiments as described in the following chapter. We are on our way to construct a more sophisticated box, deformation-cube, in which the coated objects will be placed. This cube will enable the application of exactly defined strain and/or shear deformations of the coated objects.

3.3.3 Embedding of complex structures ex vivo

First embedding experiments have been carried out using brains of cows. An one axial deformation has been applied and a MR – Image sequence has been acquired in the relaxed and deformed state respectively. In the reconstructed volumes the ROI have been pre-treated and will immediately be further evaluated.

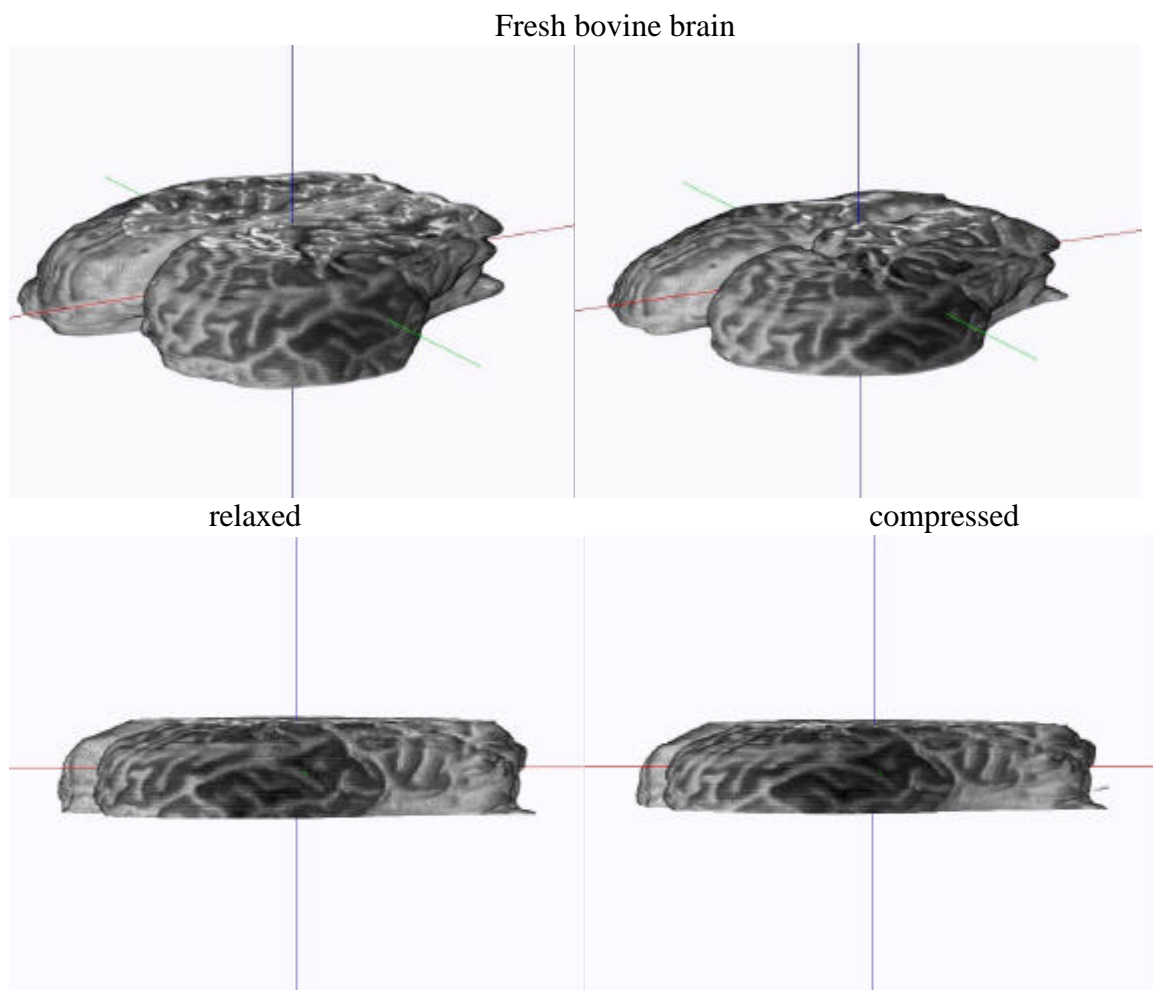


Figure 18: *Reconstruction of part of a gel-embedded bovine brain in the relaxed and deformed state.*

3.4 Advanced techniques for in vivo evaluation of tissue movement

The basic idea for in vivo measurement of structures is to use auto generated forces, forces and/or pressures which are developed in the body by itself. Thereby introduced deformation can be evaluated as established. Here the most important sources are

- heart activity with the periodic change between systolic and diastolic pressure and
- respiration which induces at least in the thorax pronounced pressure differences.

If it will be possible to quantify the induced forces and to evaluate the related deformation as developed in the preceding steps this will allow the determination of material mechanical properties.

3.4.1 MRI acquisition of dynamic deformation

Synchronisation of MRI-acquisition with spontaneous rhythms: ECG & respiration
For optimisation of image acquisition in in-vivo applications it is most important to avoid movement artefacts. For invivo image acquisition it is therefore important to synchronise the MRI machine with heart activity and /or respiration and to acquire all images at a precisely defined point in time during the cycle. In extension this technique can be used as described in the following paragraph.

Image acquisition by MRI machines can be triggered by external events. To day a standard, this possibility is mainly used for synchronisation with heart action. All images of a sequence to reconstruct a volume are taken in the same phase of subsequent cardiac cycles. So artefacts due to movement of tissue should be minimised. If one takes in the same manner volume images in different phases of the cycle of an periodically applied external force, the images can be rearranged and composed to time depending sequence of volume-images showing the dynamic response of the object under investigation to the external force. Thus one has the possibility to investigate dynamic mechanical properties also, at least to certain extent.

3.4.2 Phase contrast sequences

The big advantage of phase contrast sequences is that they provide beside the geometrical information as well information about the velocity of movement during image acquisition. In fact, to get an image two acquisitions have to be performed with a variable gradient of amplitude. By adapting the parameters to the special needs one can perform the measurements of the relatively high speed in an artery as well as the low flow movement of the cephalo-rachid liquid. So it should be possible to quantify tissue movements due too body autogenerated forces/pressures as well if a sufficient resolution is reachable.

3.4.3 Time resolving phase contrast sequences

To take first steps to investigate the possibility to apply the techniques of phase contrast for our purposes we started experiments to acquire amplitude and phase images of moving tissue. For preliminary experiments we have used the possibility to synchronize the image acquisition with the heart cycle to determine the changes in geometry of the aorta abdominalis as well as in blood velocity due to the heart cycle depending intra vascular pressure. An exemplary sequence of images of the last quarter of the heart cycle is shown in Figures 19 and 20. The change in vessel diameter can be seen by the changing size of the central white spot in the amplitude images, the increase in blood velocity is expressed by the increasing grey level difference of the central black spot with his environment in the phase images.

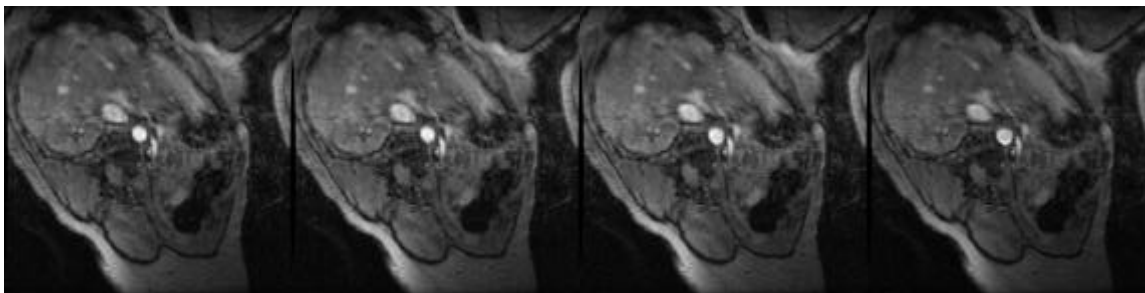


Figure 19: Heart action synchronized amplitude images of the aorta abdominalis during the last quarter of the heart cycle.

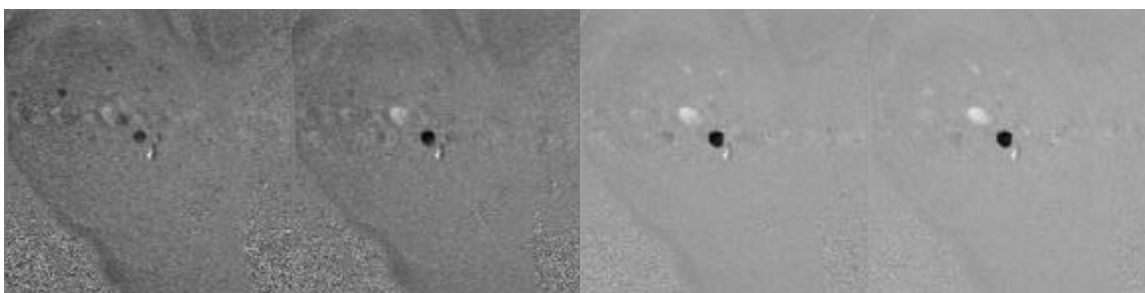


Figure 20: Heart action synchronized phase images of the aorta abdominalis during the last quarter of the heart cycle.

Further investigations to verify the possibilities to apply these techniques directly for our purposes are under way.

4 Bio-electrical material data acquisition

4.1 MR technique called Diffusion Tensor Imaging (DTI)

For the *bioelectric part of the material data generation*, a novel MR technique called Diffusion Tensor Imaging (DTI) approach will be utilised to generate material data. DTI images of a BOI (especially the human head and for model validation purposes the animal head) will be measured to generate an anisotropic conductivity map. The relation between the water diffusion tensor and the conductivity tensor in various materials and tissue types can be derived from the mathematical theory of homogenisation, especially the theory of porous media and the effective medium. This relation depends on geometric aspects of the considered materials, on cell membrane properties and intra- and extracellular coefficients. Different approaches for the calculation of the conductivity map from measured water diffusion tensor images will be implemented to satisfy the special needs of various materials and tissue types.

MPI has already implemented different sequences for DTI-measurements in the human and its associate BMZ will further implement and test sequences which are especially designed for animal head DTI.

Further details are to be found in the Design reports and reports of WP7.1.

4.2 Computation of tissue conductivities from MEG/EEG/ECOG measurements

Computation of tissue conductivities from MEG/EEG/ECOG measurements will be realized with the resulting software of work package 4. This software will be especially tailored for the analysis of our work.

4.3 Diffusion tensor scans

The conductivity tensor describes the direction dependency of the conductivity, which is also known as anisotropy. Generally, it is an asymmetric second-rank tensor (3 x 3 matrix in the three-dimensional case). Ohm's law describes the coupling between the current density vector. It can be shown that for our application the conductivity tensor can be reduced to a symmetric tensor. Further, each symmetric second-rank tensor can be transformed to a diagonal form by choosing adequate co-ordinate axes.

The lack of a technique for robust measurement of the electrical conductivity tensor *in vivo* has discouraged the inclusion of anisotropic conductivity information in the electromagnetic source imaging forward model. Recently, however, investigators have proposed a framework for inferring the electrical conductivity tensor from the spin self-diffusion tensor as measured by diffusion tensor magnetic resonance imaging. The approach essentially derives the cross-property relationship between the conductivity and diffusion tensors through an effective medium representation of the tissue geometry. In the limit of small intracellular diffusion, the cross-property relation predicts a linear relationship between the conductivity and diffusion tensors. Hence, the first-order approximation to the full effective medium relation will be employed within the project.

Based on existing human diffusion tensor scan parameters we will adapt and optimise these parameters in order to perform diffusion tensor scans on rabbits.

4.4 Development of an individual conductivity tensor map

Multimodal MR-imaging strategies in combination with high level registration and segmentation algorithms and the application of the mathematical homogenisation theory to the voxel-wise measured, anisotropic water diffusion leads to an individual conductivity tensor map of the considered BOI. This map accounts for an exact representation of various tissue types with regard to their specific anisotropic resistance, a prerequisite for modelling in e.g. EEG and MEG (see also Introduction to Biomagnetism). Pathological conditions such as e.g. skull holes and brain lesions like tumours or cerebral ischemia, strongly changing the resistance of the involved head tissues, can now be modelled individually and appropriately. This material modelling is highly innovative compared with today's volume conductor models (e.g based on the boundary element method), where e.g. the head layers brain, skull and scalp can only be assigned constant and isotropic resistance values. This will improve the diagnostic performance of EEG and MEG and will have a large impact not only on basic and clinical research but also on patient outcome in a variety of diseases.

5 Bio-material database

5.1 Literature-based data

It turns out that the biggest problem in data collection and presentation is the big variety of methods and boundaries used to determine soft tissue material properties. Since there are no standards every investigator has to and will define his own method. Boundaries as static – dynamic loads, application and kind and degree of preload, type and range of dynamic force/strain applied, and most important the way of tissue sample harvesting and treatment before experimental evaluation. These experimental conditions are chosen individually depending on the special interest of the project.

This diversity is the reason that experimental data reported in literature is hardly comparable and has to be evaluated in a most critical manner to assure relevance for the here intended use in modelling and simulation of soft tissue. In the appendix we present the most appropriate data collected so far. Further evaluation and verification will be necessary and carried out in light of our own experiments that will be performed in the upcoming project phase. Major attention will be taken in regard to anisotropy of mechanical properties, which until now rarely has been taken into account. The data presented in the Appendix include properties of a variety of soft and hard tissue mainly that to be found in the neuro-cranium.

This first general material database shall provide the basis for the initial simulations performed in WP7.

5.2 Database

5.2.1 Data presentation

The structure of the material database will be adapted to the needs of the different modelling and simulation activities in the project and facilitate rapid inclusion of new data for extended applications. The database format will be defined in conjunction with the interfacing activities of WP 6. Anyway since we start already with a first preliminary data base in this report that is based on literature values only. So, at the moment we have adapted the way of data presentation to the one used generally in literature. Here data is most often given as single values which are evaluated under specific boundary conditions. If the nonlinearity of stress-strain relationship is taken into account also, the data is most often represented in graphs. Anisotropy is normally not treated in a systematic way.

Our data elevation and presentation will be done in different steps. Most reasonable boundary conditions will be chosen and particular experiments will be performed resulting in single

values. If possible and reasonable anisotropy will be taken into account also and the data will be presented in tensor form.

This will be done for the exvivo traction experiments as well as for MRSI and as far as realisable for invivo MRSI. For traction experiments this can and will be done for the both, static and dynamic load.

Investigation of dynamic properties will be done in the next future by our traction machine treating small samples of tissue exvivo. While this data will be published in one of the next edition of our data base, it will not be possible during the runtime of the project to perform dynamic experiments by the invivo MRSI method.

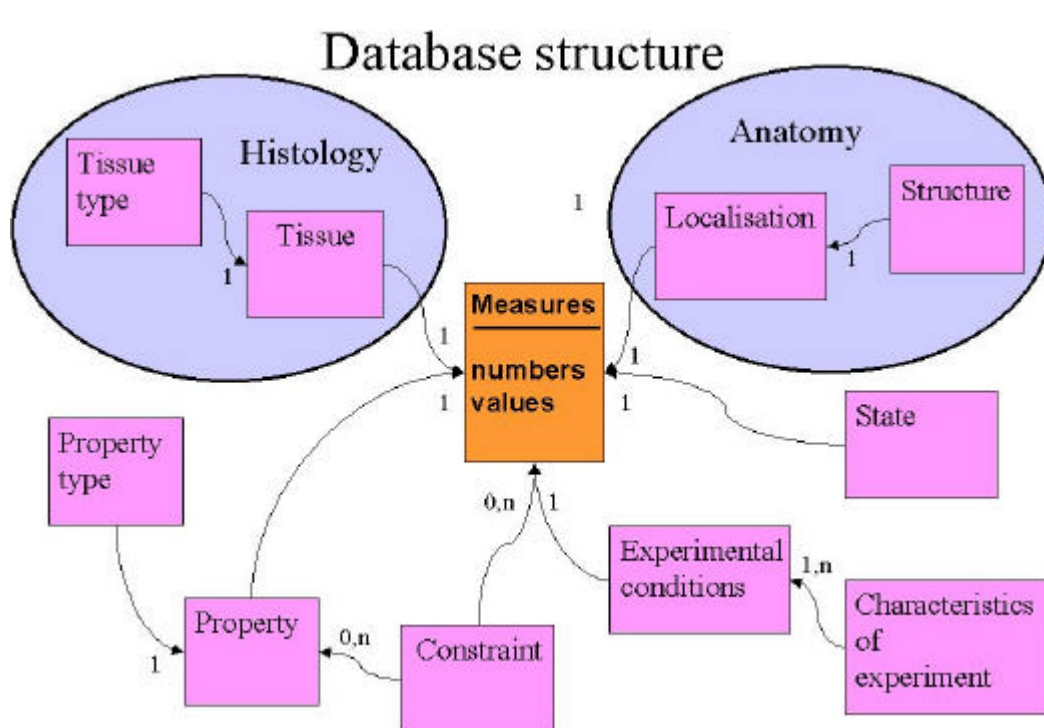


Figure 21: Structure of datase in 'Access'.

5.2.2 Data encoding

To facilitate access and use of the database a tissue property classification scheme will be invented. A code will be used which identifies:

- type of tissue: bone, muscle,
- material properties characteristics: linear, static, isotrop, ...
- way of sample preparation: invivo, deep frozen,
- type of experimental setup used: traction machine, US, ...

This code will have the following form:

XXX-xxxx-XXXX-xxxx

It will accompany every material property value given, to enable simple choice of adequate data for a special model. This type of presentation will augment the transparency of given data and should allow to compare values from different sources in a more easy and meaningful way.

We aim to present the complete code description and the first version of our encoded database in the next database release.

6 Literature

- [Bil98] Bilgen M, Insana MF
Elastostatics of a spherical inclusion in homogeneous biological media.
Phys Med Biol 1998 Jan;43(1):1-20
- [Che98] Chenevert TL, Skovoroda AR, O'Donnell M, Emelianov SY
Elasticity reconstructive imaging by means of stimulated echo MRI.
Magn Reson Med 1998 Mar;39(3):482-90
- [Doy00] Doyley MM, Meaney PM, Bamber JC
Evaluation of an iterative reconstruction method for quantitative elastography.
Phys Med Biol 2000 Jun;45(6):1521-40
- [Eme95] Emelianov SY
Elasticity imaging for early detection of renal pathology.
Ultrasound Med Biol. 1995;21(7):871-83.
- [Erk98] Erkamp RQ, Wiggins P, Skovoroda AR, Emelianov SY, O'Donnell M
Measuring the elastic modulus of small tissue samples.
Ultrason Imaging. 1998 Jan;20(1):17-28.
- [Fow95] Fowlkes JB, Emelianov SY, Pipe JG, Skovoroda AR, Carson PL, Adler RS, Sarvazyan AP
Magnetic-resonance imaging techniques for detection of elasticity variation.
Med Phys 1995 Nov;22(11 Pt 1):1771-8
- [Fun93] Fung Y.C.
Biomechanics: Mechanical Properties of Living Tissues.
2nd ed., Springer-Verlag, New York, Berlin, Heidelberg, 1993
- [Gow89] Gowland PA
The use of an improved inversion pulse with the spin-echo/inversion-recovery sequence to give increased accuracy and reduced imaging time for T1 measurements.
Magn Reson Med. 1989 Nov;12(2):261-7.
- [Kal96] Kallel, F.; Bertrand, M.
Tissue elasticity reconstruction using linear perturbation method
Medical Imaging, IEEE Transactions on : pp. 299 – 313, Vol.15(3), June 1996
- [Mil97] Miller K, Cinzei K
Constitutive Modelling of Brain Tissue – Experiment and Theory
J.Biomechanics, Vol.30, 11/22, pp.1115-1121, 1997
- [Oph99] Ophir J, Alam SK, Garra B, Kallel F, Konofagou E, Krouskop T, Varghese T
Elastography: ultrasonic estimation and imaging of the elastic properties of tissues.
Proc Inst Mech Eng [H] 1999;213(3):203-33
- [Rob96] Robson MD, Constable RT

Three-dimensional strain-rate imaging.
Magn Reson Med 1996 Oct;36(4):537-46

[Sum95] Sumi C, Suzuki A, Nakayama, K
Estimation of shear modulus distribution in soft tissue from strain distribution.
IEEE Trans Biomed Eng 1995 Feb;42(2):193-202

[Zhu99] Zhu Y, Chaturvedi P, Insana MF
Strain imaging with a deformable mesh.
Ultrason Imaging 1999 Apr;21(2):127-46

Appendix

7 Mechanical tissue properties

7.1 Soft tissue

Table 1: Mechanical properties of tissues of the neuro-cranium regarding linear elasticity

Author	Substructures ¹	E (kPa)	G (kPa)	K (kPa)	ρ (kg/m ³)	n	tan (δ)
Lee [1987] Lighthall [1989] Ueno [1989,1991]			80.0		1000	0.475 & 0.49	0.2
Lee [1990]	brain (gel) ²	80.0- 121.2				0.49	
Chu [1991]	skull Brain	6.5×10^6 250.0			2027 1000	0.2 0.49	0.001 0.001
Ruan [1991a]	Skull Brain dura, falx, tentorium CSF	6.5×10^6 66.7 31.5×10^5 66.7		2.19×10^8 - 2.19×10^6	1412 1040 1133 1040	0.22 0.48 - 0.49999492 0.45 0.499	
Ruan [1991b]	outer table Diploe inner table Brain CSF		5.0×10^6 2.32×10^6 5.0×10^6 1.68×10^7 500	7.3×10^9 3.4×10^6 7.3×10^9 2.19×10^3 2.19×10^4	3000 1750 3000 1040 1040	0.22 0.22 0.22 0.4996 0.489	
Ruan ³ [1992]							
Trosseille [1992]	Brain CSF	240.0			1000	0.49 - 0.499 0.49999	0.2
Willinger [1992]	Skull Brain Subarachnoid space	5×10^6 675.0 5×10^{-2}				0.2 0.48 0.49	

E : Young's modulus ; G : shear modulus ; K : bulk modulus ; ρ : density ;
v : Poisson ratio ; tan(δ) : loss tangent

¹ skull is not mentioned if rigid

² in 2-D and 3-D full-cylinder model

³ no values given, probably identical to Ruan [1991b]

Table 2: Mechanical properties of tissues of the neuro-cranium regarding linear viscoelasticity

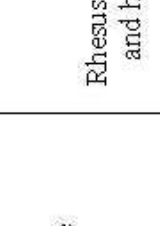
Author	Substructures	E (kPa)	G_{∞} (kPa)	G_0 (kPa)	b (s ⁻¹)	ρ (kg/m ³)	n	K (MPa)
Galbraith [1998] Tong [1989]	brain (gel)		5.512	11.02	200		0.4995	
Cheng [1990]	brain (gel)		16.2	49.0	145		≈ 0.5	
Lee [1990]	brain (gel) ¹ CSF/ventricles ²		2.87 - 18 3 - 6	26.9 - 110 9 - 24	50 50	950		1.25 - 5.44 0.445
DiMasi [1991a, 1991b]	Skull Brain Dura	2.4×10^6 6890	17.225	34.45	100			0.0689

E : Young's modulus ; G_{∞} : static shear modulus ; G_0 : dynamic shear modulus ;
 β : decay constant ; ρ : density ; v : Poisson ratio ; K : bulk modulus

¹ used in half-cylinder, full-cylinder and skull physical models of Margulies [1987]

² used in skull physical models of Margulies [1987]

Table 3: Special data of mechanical properties of tissues of the neuro-cranium

Author	Description of experiment	Specimens	Temperature (°C)	Parameters calculated	Results
(Franke 1954)	Vibrating sphere into brain homogenate and whole brain (f = 150, 125 and 500 Hz)	Fig brain	22	Viscosity	14.9P
(Dodgson 1962)	Creep	Mouse brain	26		Strain = $K \times \log(t)$ (t=time) Creep $\rightarrow E(t) = K \times \log(t)$ (E = strain, K = constant)
(Koenenman 1966)	<ul style="list-style-type: none"> Creep Vibration (80 \rightarrow 350 Hz) 	Rabbit, calf and pigs white matter	22	Elastic modulus	Vibration \rightarrow 0.8 < Elastic modulus < 1.5 dynes/cm ²
				Viscosity	Vibration \rightarrow Dynamic viscosity = 43.5P
(Ormmaya 1968)	Fall of a sphere into brain homogenate	Rhesus monkey and cat brains	10-15	Viscosity	407P
				Empirical creep compliance function: $J(t) = C1 + C2 \times \ln(t)$ Creep response: Four parameter Maxwell-Kelvin model	Human Monkey 3.55×10^{-1} 4.3×10^{-1} 2.60×10^{-2} 2.59×10^{-2}
					E_1 (psi) 3.4 E_2 (psi) 9.3 η_2 (lb-sec/in ²) 257.4 η_3 (lb-sec/in ²) 8.6 9.7
(Galford and McElhaney 1970)	<ul style="list-style-type: none"> Creep compliance Relaxation Free vibration 	Rhesus monkey and human		Free vibration: $E^* = E_1 + iE_2$	E_1 (psi) 9.68 E_2 (psi) 3.80 ω (Hz) 34.0 E^* (psi) 10.4 Relax. modulus (t=0) (psi) 15.3 1.5 0.95

Note : 1 dyne (cm² gm/s²) = 0.00001 N (force), 1 poise = 1.00000 kg/m/s, 1 pound = 0.45359237 kg, 1 psi = 6894.757 Pa

Cartilage

Table 4: Mechanical properties of articular cartilage

Author	Articular cartilage	
	Poisson Ratio ν	Young's Modulus E (MPa)
Schreppers & Sauren [1990]	0.4	10
Lengsfeld [1993]	0.35	100
Bendjaballah et al. [1995]	0.45	12
Bendjaballah et al. [1997]	0.45	12

R = structure modelled as rigid

Table 5: Mechanical properties of meniscus

Author	Isotropic Meniscus		Meniscus Matrix		Meniscal Fibres		Transverse isotropic meniscus	
	Poisson Ratio ν	Young's Modulus E (MPa)	Poisson Ratio ν	Young's Modulus E (MPa)	Poisson Ratio ν	Young's Modulus E (MPa)	Poisson Ratio ν	Young's Modulus E (MPa)
Sauren et al. [1984]	0.3	20/200						
Hefzy et al. [1987]	0.3	20/200						
Fithian et al. [1990] *		Parallel	90°					
		60	60					
		198	2.8					
		138	4.6					
Schreppers & Sauren [1990]	0.3	20					$\nu_{12} = 5.0$ $\nu_{23} = 0.3$	$E_1 = 50 / 20$ $E_2 = 10 / 5$
Spilker et al. [1992]							$\nu_{12} = 2.0$ $\nu_{23} = 0.05$	$E_1 = 200$ $E_2 = 0.055$
Lengsfeld [1993]	0.35	50/5						
Bendjaballah et al. [1995]			0.45	8		170 (deep) 60 (superficial)-		
Bendjaballah et al. [1997]			0.45	8		170 (deep) 60 (superficial)-		

7.2 Hard tissue**Table 6:** Mechanical properties of cortical and cancellous bone

Author	Cortical bone		Cancellous bone	
	Poisson Ratio ν	Young's Modulus E (MPa)	Poisson Ratio ν	Young's Modulus E (MPa)
Sauren et al. [1984]	0.2	500 / 5000	NG	NG
Hefzy et al. [1987]	0.2	500 / 5000	NG	NG
Schreppers & Sauren [1990]	0.2	500	NG	NG
Lengsfeld [1993]	0.35	10000	0.35	1000
Bendjaballah et al. [1995]	R	R	R	R
Bendjaballah et al. [1997]	R	R	R	R

R = structure modelled as rigid

NG = information not given

8 Electrical tissue properties

8.1 Soft tissue

8.1.1 Brain matter, spinal cord, and cerebellum

Table 7: Resistivity of brain white matter

Author	Animal	Frequency (Hz)	Pulse (ms)	Resistivity (W.cm)	
Crile et al. [1922]	Rabbit	1000		746	
Van Harreveld et al. [1963]	Rabbit	1000		957	
Nicholson [1965]	Cat	20		Normal	850
				Parallel	89
Freygang and Landau [1955]	Cat		0.3 → 0.7	333 (isotropic resistivity)	

Table 8: Resistivity of brain grey matter

Author	Animal	Frequency (Hz)	Pulse (ms)	Resistivity (W.cm)
Freygang and Landau (1955)	Cat		0.3 → 0.7	222
Van Harreveld et al. (1963)	Rabbit	1000		208
Ranck (1963)	Rabbit	5		321
Crile et al. (1922)	Rabbit	1000		438

Table 9: Resistivity of spinal cord

Author	Animal	Frequency (Hz)	Pulse (ms)	Resistivity (W.cm)	
Crile et al. [1922]	Rabbit	1000		576	
Ranck [1963]	Cat	5-10		Normal	1211
				Parallel	175

Table 10: Resistivity of cerebellum

Author	Animal	Frequency (Hz)	Pulse (ms)	Resistivity (W.cm)
Crile et al. [1922]	Rabbit	1000		730

8.1.2 Muscle

Table 11: Resistivity of muscle

Author	Specimen	Frequency (Hz)	Pulse (ms)	Resistivity (W.cm)	
Burger and van Dongen	Rabbit muscle			Longitudinal	125
				Transverse	1800
Rush et al. [1963]	Human arm muscle		100	Longitudinal	150
				Transverse	3000
Geddes and Baker [1967]					
Polk and Postow [1986]					

8.1.3 Fat

Table 12: Resistivity of fat

Author	Animal	Frequency (Hz)	Pulse (ms)	Resistivity (W.cm)
Rush et al. [1963]			100 *	2500
Schwan and Kay [1956]	Dog	1000		1500 → 5000

* = d.c.

8.1.4 Scalp

Table 13: Resistivity of scalp

Author	Specimen	Frequency (Hz)	Pulse (ms)	Resistivity (W.cm)
Geddes and Baker [1967]	Human scalp		*	230

* = d.c.

8.2 Bone

Table 14: Resistivity of bone

Paper	Specimen	Frequency (Hz)	Pulse (ms)	Resistivity (W.cm)	
Geddes and Baker [1967]	Thorax bone	low		16000	
Reddy and Saha [1984]	Wet bovine bone	10000		Axial	16600
				Circumferential	36000
				Radial	54000

8.3 Fluids

8.3.1 Blood

Table 15: Resistivity of blood

Author	Specimen	Frequency (Hz)	Pulse (ms)	Resistivity (W.cm)
Rush et al. [1963]		low		162

8.3.2 Cerebrospinal fluid

Table 16: Resistivity of cerebrospinal fluid

Author	Subject	Frequency (Hz)	Pulse (ms)	Resistivity (W.cm)
Geddes and Baker [1967]	Human	1000 – 30 000		65

Bibliography Database

- Burger H. C. a,d Van Dongen R.** (1961) Specific resistance of body tissues. *Physics in Medicine and Biology*. 5(4) : 431-447
- Cheng L.Y., Rifai S., Khatua T. and Piziali R.L.** (1990) Finite element analysis of diffuse axonal injury. *Proc. 34th Stapp Car Crash Conf.*, SAE Paper 900547. pp 141-154
- Chu C.S. and Lee M.C.** (1991) Finite element analysis of cerebral contusion. *Advances in Bioengineering*, ASME-BED-Vol. 20, pp 601-604
- Crile G.W., Hosmer H.R., and Rowland A.F.** (1922) The electrical conductivity of animal tissues under normal and physiological conditions. *Am. J. Physiol.* 60 : 59-106
- DiMasi F., Eppinger R. H., Gabler III H.C. and Marcus J.H.** (1991a) Simulated head impacts with upper interior structures using rigid and anatomic brain models. *Auto & Traffic Safety*. Summer, pp 20-31
- DiMasi F., Marcus J., Eppinger R.** (1991b) 3-D anatomic brain model for relating cortical strains to automobile crash loading. *Proc. 13th Int. Techn. Conf. On Experimental Safety Vehicles*. November 4-7, Paper No. 91-S8-O-11.
- Dodgson, M. C. H.** (1962) Colloidal structure of brain. *Biorheology* 1: 21-30.
- Fithian D.C., Kelly M.A., Mow V.C.** (1990) Material properties and structure-function relationships in the menisci. *Clin Orthop*. Mar;(252):19-31.
- Franke, E. K.** (1954) The response of the human skull to mechanical vibrations. Wright-Patterson Air Force Base, Ohio, WADC Tech. Rept. 54-24.
- Freygang W.H. and Landau W.M.** (1955) Some relations between resistivity and electrical activity in the cerebral cortex of the cat. *J. of Cell. Comp. Physiol.* 45 : 377-392
- Galbraith C.G. and Tong P.** (1988) Boundary conditions in head injury finite element modelling. *16th Annual Int. Workshop on Human Subjects for Biomechanical Research*. pp 179-193
- Galford, J. E. and J. H. McElhaney** (1970) A viscoelastic study of scalp, brain, and dura. *J Biomech* 3(2): 211-21.
- Geddes L.A. and Baker L.E.** (1967) The specific resistance of biological materials – a compedium of data for the biomedical engineer and physiologist. *Med. And Biol. Eng.* 5 : 271-293
- Koeneman, J. B.** (1966) Viscoelastic properties of brain tissue. Unpublished M.S. Thesis, Case institute of Technology.
- Lee E.S.** (1990) A large-strain, transient-dynamic analysis of head injury problems by the finite element method. Ph.D. Dissertation, Georgia Institute of Technology

- Lee M.C., Melvin J.W. and Ueno K.** (1987) Finite element analysis of traumatic subdural hematoma. *Proc. 31st Stapp Car Crash Conf.*, SAE Paper 872201, pp 67-77
- Lengsfeld M.** (1993) Stresses at the meniscofemoral joint: elastostatic investigations on the applicability of interface elements. *J Biomed Eng.* Jul;15(4):324-8.
- Lighthall J.W., Melvin J.W. and Ueno K.** (1989) Toward a biomechanical criterion for functional brain injury. *Proc. 12th Int. Techn. Conf. on Experimental Safety Vehicles.* pp 627-633
- Nicholson P.W.** (1965) Specific impedance of cerebral white matter. *Experimental Neurology.* 13 : 386-401
- Ommaya, A. K.** (1968) Mechanical properties of tissues of the nervous system. *J. Biomech.* 1: 127-38.
- Polk Ch. And Postow E., editors** (1986) CRC Handbook of Biological Effects of Electromagnetic Fields. CRC Press
- Ranck J.B.** (1963) Specific impedance of rabbit cerebral cortex. *Experimental Neurology.* 7 : 144-152
- Ranck Jr. J.B. and Be Merit S.L.** (1965) The specific impedance of the dorsal columns of the cat; an anisotropic medium. *Experimental Neurology.* 11 : 451-463
- Reddy G.N. and Saha S.** (1984) Electrical and dielectric properties of wet bone as a function of frequency. *IEEE Transactions on Biomedical Engineering.* 31(3) : 296-302
- Ruan J.S., Khalil T. and King A.I.** (1991a) Human head dynamic response to side impact by finite element modeling. *J. Biomechanical Engineering.* Vol. 113, pp 276-283
- Ruan J.S., Khalil T. and king A.I.** (1991b) Intracranial response of a three-dimensional human head finite element model. *Proc. Injury Prevention through Biomechanics Symposium,* Wayne State University. Pp 97-103
- Ruan J.S., Khalil T. and King A.I.** (1992) Finite element analysis of the human head to impact. *Advances in Bioengineering,* ASME-BED-Vol. 22, pp 249-252
- Rush S., Abildskov J.A., and McFee R.** (1963) Resistivity of body tissues at low frequencies. *Circulation Research.* 12 : 40-50
- Schreppers G.J., Sauren A.A., Huson A.** (1990) A numerical model of the load transmission in the tibio-femoral contact area. *Proc Inst Mech Eng [H].* 204(1):53-9.
- Schwan H.P. and Kay C.F.** (1956) Specific resistance of body tissues. *Circulation research.* 4 : 664-670
- Tong, DiMasi, Carr, Eppinger, Marcus and Galbraith** (1989) Finite element modeling of

head injury caused by inertial loading. *Proc. 12th Int. Conf. On Experimental Safety Vehicles*. pp 617-626

Trosseille X., Tarrière C., Lavaste F., Guillon F. and Domont A. (1992) Development of a F.E.M. of the human head according to a specific test protocol. *Proc. 36th Stapp Car crash Conf.*, SAE Paper 922527, pp 235-253

Ueno K., Melvin J.W., Lundquist E. and Lee M.C. (1989) Two-dimensional finite element analysis of human brain impact responses : Application of a scaling law. *Crashworthiness and Occupant Protection in Transportation Systems*, AMD-Vol. 106/ BED-Vol. 13, Ed.: Khalil T.B., ASME, 1989, pp 123-124

Ueno K., Melvin J.W., Rouhana M.E. and Lighthall J.W. (1991) Two-dimensional finite element model of the cortical impact method for mechanical brain injury. *Crashworthiness and Occupant Protection in transportation Systems*, AMD-Vol. 126/BED-Vol. 19, ASME, 1991, pp 121-147

Van Harreveld A., Murphy T., and Nobel K.W. (1963) Specific impedance of rabbit's cortical tissue. *Am. J. Physiol.* 205 : 203-207

Willinger R., Kopp C.M. and Césari D. (1992) New concept of contrecoup lesion mechanism : modal analysis of a finite element model of the head. *Proc. Int. IRCOBI Conf. on the Biomechanics of Impacts*. pp 283-297